The Nonlinear Evolution of Ion Cyclotron Waves in the Earth's Magnetosheath*

GUO Jun (郭俊)[1,2], YANG Zhongwei (杨忠炜)[3], LU Quanming (陆全明)[2,3], WANG Shui (王水)[3]

[1]School of Mathematics and Physics, Qingdao University of Science and Technology, Qingdao 266042, China
[2]State Key Laboratory of Space Weather, Center for Space Science and Applied Research, Chinese Academy of Sciences, Beijing 100080, China
[3]School of Earth and Space Sciences, University of Science and Technology of China, Hefei 230026, China

Abstract With one-dimensional (1-D) hybrid simulations we investigate the nonlinear evolution of the ion cyclotron waves excited by the H^+ and He^{2+} temperature anisotropies, and analyze the evolution by using the wavelet analysis method. The results show that the proton cyclotron waves with the dominant frequency higher than the helium gyro-frequency ($\Omega_{\rm He} = 0.5\Omega_{\rm p}$, with $\Omega_{\rm p}$ and $\Omega_{\rm He}$ the proton and helium gyro-frequencies respectively) are firstly excited, and then the helium cyclotron waves with the dominant frequency lower than the helium gyro-frequency are excited. The relation of our simulation results to the BIF(bifurcated) (there are two peaks in the wave spectrum: one above and one below $\Omega_{\rm He}$) and CON(continuous) (continuous spectrum from 0.1 $\Omega_{\rm p}$ to 1.0 $\Omega_{\rm p}$) wave spectra observed in the magnetosheath are discussed.

Keywords: ion cyclotron wave, hybrid simulation, temperature anisotropy

PACS: *52.35.Hr, 52.65.Ww*

1 Introduction

Analytical theory and hybrid simulations predicted that ion temperature anisotropies can excite both ion cyclotron waves and compressive mirror waves [1∼4]. Adjacent to the sunward side of the low-shear dayside magnetopause, there exists a region characterized by a reduced plasma density and increased magnetic field strength. This region is called the plasma depletion layer(PDL), which is formed by the stretching of the magnetic field lines and the consequent pileup of the magnetic field as the magnetosheath plasma approaches the magnetopause [5,6]. Spacecraft observations showed that there is a wide variety of magnetic fluctuations in the PDL. The magnetic fluctuations are predominantly transverse to the background field and their frequencies can be up to the proton gyrofrequency. Detailed analysis shows that the fluctuations are mainly electromagnetic ion cyclotron waves excited by the H^+ and He^{2+} temperature anisotropies [7∼9]. However, in PDL the proton plasma beta $\beta_{\rm p}$ is usually below one, and in such a situation the magnetic fluctuations excited by the temperature anisotropies are mainly ion cyclotron waves while the compressive mirror-mode waves can be neglected [7,10]. One of the possible mechanisms for such temperature anisotropies is due to the heating of the quasi-perpendicular shock [11,12] and observations indicated that PDL is preferentially formed when the upstream shock is quasi-perpendicular [13]. In addition to this mechanism, both the perpendicular compression of flux tubes at the magnetopause and flux tube stretching along the magnetic field around the magnetopause may also drive the temperature anisotropies [14,15].

Besides these, AMPTE/CCE(active magnetic particle track explorer/ charge composition explorer) and Wind spacecraft observed that the ion cyclotron waves inside PDL have three different spectral categories, namely LOW(low), CON(continuous) and BIF (bifurcated) spectrum, respectively. ANDERSON et al. [8] defined these categories as follows. LOW is a continuous spectrum of the ion cyclotron waves with their main power appearing below 0.5 $\Omega_{\rm p}$ with $\Omega_{\rm p}$ the proton gyrofrequency; CON is a continuous spectrum with the main power appearing from ∼0.1 $\Omega_{\rm p}$ to 1.0 $\Omega_{\rm p}$; BIF is a spectrum which is characterized by two activity peaks, above and below 0.5 $\Omega_{\rm p}$, respectively. With the linear Vlasov theory, DENTON et al. [16] found that for low parallel proton plasma beta $\beta_{//p}$ there exist two frequency bands in the spectrum of the excited ion cyclotron waves, and it can explain the BIF category observed in PDL. The higher-frequency band is driven by H^+ temperature anisotropy, while the lower-frequency band is driven by He^{2+}. With the increase in $\beta_{//p}$, two unstable frequency bands merge and form a continuous wave spectrum, which can explain the CON category observed in PDL. It was also found with the

*supported by National Natural Science Foundation of China (Nos. 40725013, 40674093), and the Open Research Program Foundation of State Key Laboratory for Space Weather, Chinese Academy Sciences

linear Vlasov theory that a relative velocity between H^+ and He^{2+} can eliminate the gap between the two frequency bands in BIF and forms a continuous spectrum [17]. The above results are based on the linear Vlasov theory which can only study the linear stage of the ion cyclotron waves. Hybrid simulations can be used to study the nonlinear evolution of the ion cyclotron waves excited by the temperature anisotropies of both H^+ and He^{2+} [18]. CAO et al. [19,20] studied the instabilities driven by non-gyrotropic ring ions by means of one-dimensional (1-D) electromagnetic hybrid computer simulations, and found that newborn protons, injected into the system with a specified initial pitch angle of 90°, can excite almost invariable low frequency waves and the perpendicular velocity of the newborn ions generally decreases due to the energy diffusion resulting from wave-particle interaction. LU et al. [21] investigated the spectrum evolution of the ion cyclotron waves with the fast Fourier transformation (FFT) method. However, the FFT method can only study the integral effect, and explore when the wave appears and how it evolves with the time. In this study, with 1-D hybrid simulations we investigate the ion cyclotron waves excited by the H^+ and He^{2+} temperature anisotropies, and analyze the nonlinear evolution of their wave spectrum with the wavelet analysis method. The wavelet transformation is a powerful tool, which can analyze time series containing non-stationary power with different frequencies.

2 Simulation model

In the hybrid simulations the ions are treated kinetically while the electrons are considered as massless fluid [11]. The plasma consists of two ion components (proton and He^{2+}) and the electron component. Initially, both proton and He^{2+} are assumed to be of bi-Maxwellian velocity distribution which bears a zero average flow velocity, and with the same thermal velocity in the direction parallel to the background magnetic field. Periodic boundary conditions for the particles and fields are used in the simulations. The background magnetic field is assumed to be $\mathbf{B}_0 = B_0\mathbf{x}$. In the simulations, the units of space and time are $c/\omega_{\rm pp}$ (where $c/\omega_{\rm pp}$ is the proton's inertial length) and $\Omega_{\rm p}^{-1}$ (where $\Omega_{\rm p} = eB_0/m_{\rm p}$ is the proton's gyro frequency). In 1-D hybrid simulations, the number of the grid cells is $n_x = 256$, and the grid size is $\Delta x = 1.0\ c/\omega_{\rm pp}$ with 500 particles per cell for each ion component. The time step is taken to be $\Omega_{\rm p}t = 0.02$. The simulations are performed in the center-of-mass frame, where the charge neutrality and the zero current condition are imposed at $t = 0$. In the simulations, the values of temperature anisotropies $T_\perp/T_{//}$, with $//$ and $\perp$ the directions parallel and perpendicular to the ambient magnetic field respectively, for proton and He^{2+} are 3.8 and 4.56, respectively. The relative number density of He^{2+} is $\eta = n_\alpha/(n_\alpha + n_{\rm p}) = 0.04$ with $n_{\rm p}$ and n_α the number density of proton and He^{2+}, respectively. Two plasma beta values are chosen as (a) $\beta_{//\,p} = 0.15$ and (b) $\beta_{//\,p} = 0.5$.

3 Simulation results

With 1-D hybrid simulations we investigate the ion cyclotron waves excited by the H^+ and He^{2+} temperature anisotropies, and analyze the nonlinear evolution of their spectrum by using the wavelet analysis method. Fig. 1 shows the time evolution of H^+ and He^{2+} temperature anisotropies for run (a). Both the H^+ and He^{2+} temperature anisotropies decrease with the excitation of the ion cyclotron waves. Therefore the ion cyclotron waves include the proton cyclotron waves and helium cyclotron waves, excited by the H^+ and He^{2+} temperature anisotropy, respectively. The helium cyclotron waves are excited later than the proton cyclotron waves because He^{2+} has a smaller charge-to-mass ratio than H^+. The H^+ temperature anisotropy begins to decrease rapidly at $\Omega_{\rm p}t \sim 20$, and almost reaches a constant at $\Omega_{\rm p}t \sim 100$. The He^{2+} temperature anisotropy begins to decrease rapidly at $\Omega_{\rm p}t \sim 100$, and a constant is reached at $\Omega_{\rm p}t \sim 200$. In the quasi-equilibrium stage, the H^+ and He^{2+} temperature anisotropies are about 2.75 and 2.5, respectively.

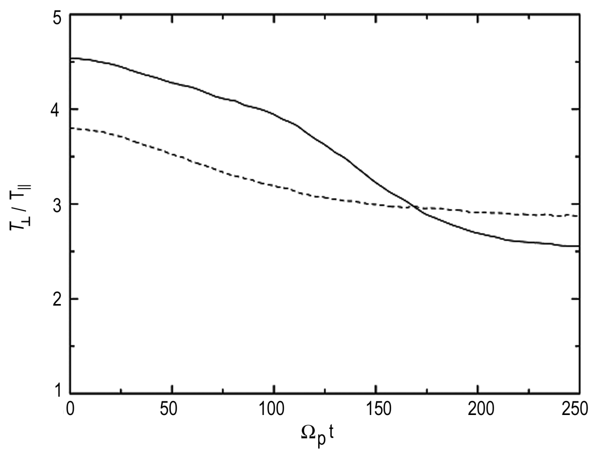

Fig.1 Time evolution of the H^+ and He^{2+} temperature anisotropies for run (a). The solid and dash lines represent He^{2+} and H^+, respectively

Fig. 2 presents the spectrum evolution of the excited waves by the wavelet method. The left axis is the wave frequency and the bottom axis is time with the unit of $\Omega_{\rm p}^{-1}$. The thick dashed contour encloses the regions of beyond 99% confidence. The region below that indicates the cone of influence, where the edge effects become important. The spectrum is calculated through the following procedures. We first calculate the wavelet power spectrum of the time series of the fluctuating magnetic filed B_y at each grid point, and the spectrum shown in Fig. 2 is the average value of all the grid points. We can find that the waves excited during the period from $\Omega_{\rm p}t \sim 50$ to 190 are the proton cyclotron waves, and their dominant frequency is about 0.62 $\Omega_{\rm p}$.

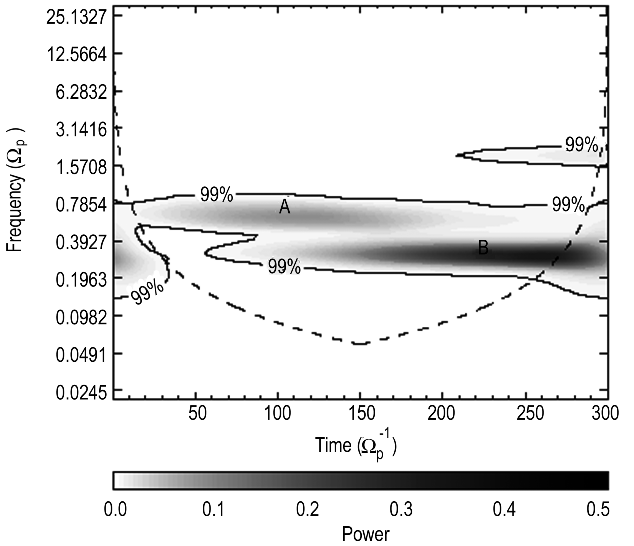

Fig.2 Local wavelet power spectrum of the time series of B_y for run (a)

Helium cyclotron waves with the dominant frequency around 0.3 Ω_p are excited at $\Omega_\mathrm{p}t$ ~100. Therefore, there exist two frequency bands in the spectrum during the period from $\Omega_\mathrm{p}t$ ~100 to 190. The spectrum is similar to the BIF spectral category observed by AMPTE/CCE [8] and Wind spacecraft [10] in the PDL. At $\Omega_\mathrm{p}t$ ~200, the frequency band corresponding to the proton cyclotron waves disappears, and only the band corresponding to the helium cyclotron waves remains. The main power in the spectrum appears below the helium gyrofrequency, which is similar to the LOW category observed in the magnetosheath [8]. The excited waves are symmetric along the $+x$ and $-x$ directions, and they have the same polarization. We can separate the waves into the parts which propagate along the $+x$ and $-x$ directions [11]. In Fig. 3, we show the polarization of the waves which propagate in the $+x$ direction. It can be found that the waves are left-hand circularly polarized.

Fig. 4 is the distribution of the frequency at different times for run (a), where A, B, C, and D represent $\Omega_\mathrm{p}t = 50$, 80, 150, 220, respectively. There are only the proton cyclotron waves with a dominant frequency around 0.62 Ω_p at time A. Then the amplitude of the proton cyclotron waves continue to increase and the helium cyclotron waves appear at time B. There exist two frequency bands in the spectrum at time C, both the dominant frequency and the amplitude of the proton cyclotron waves decrease a little. Only the helium cyclotron waves with a dominant frequency around 0.3 Ω_p exist at time D.

Fig. 5 shows the time evolution of proton and He^{2+} temperature anisotropies for run (b). Similar to run (a), the H^+ temperature anisotropy first decreases, and then the He^{2+} temperature anisotropy decreases. The proton temperature anisotropy begins to decrease at about $\Omega_\mathrm{p}t = 10$, and reaches almost a constant at about $\Omega_\mathrm{p}t = 50$. The He^{2+} temperature anisotropy begins to decrease at about $\Omega_\mathrm{p}t = 50$, and a constant is reached

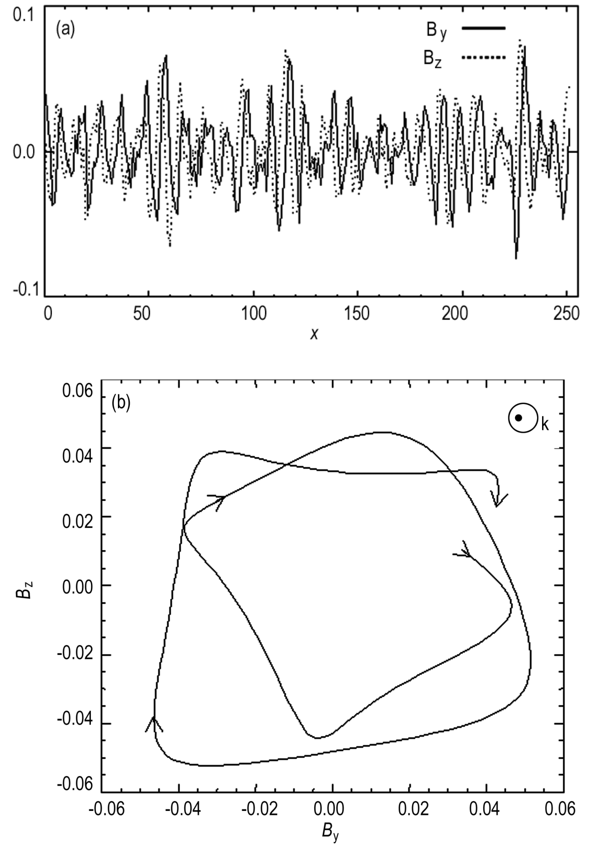

Fig.3 (a) Spatial distribution of the magnetic fields at $\Omega_\mathrm{p}t = 80$. (b) Hodograph of the magnetic fields at $nx = 1$ and with the time interval $\Omega_\mathrm{p}t$ from 60 to 80

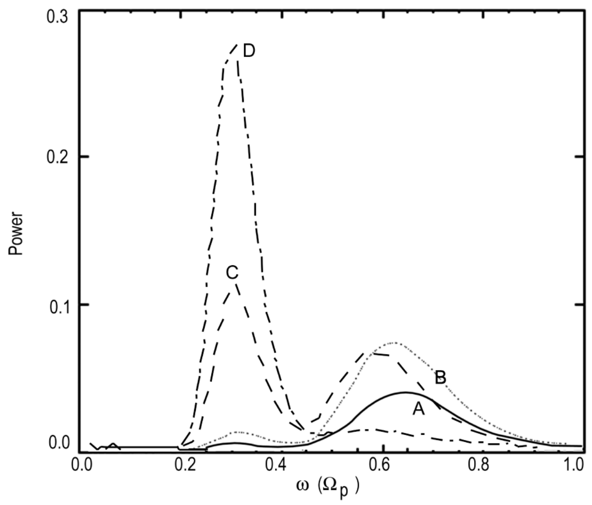

Fig.4 Frequency spectrum of the excited ion cyclotron waves at different times for run (a). The solid(A), dotted(B), dashed(C) and dash-dotted(D) lines represent $\Omega_\mathrm{p}t = 50$, 80, 150, 220, respectively

at about $\Omega_\mathrm{p}t = 100$. In the quasi-equilibrium stage, the proton and He^{2+} temperature anisotropies are about 1.5 and 1.7, respectively.

Shown in Fig. 6 is the wavelet power spectrum of the time series of B_y for run (b). It is clearly seen that the increase in the thermal velocity broadens the spectrum of the excited waves. During the first stage, the proton

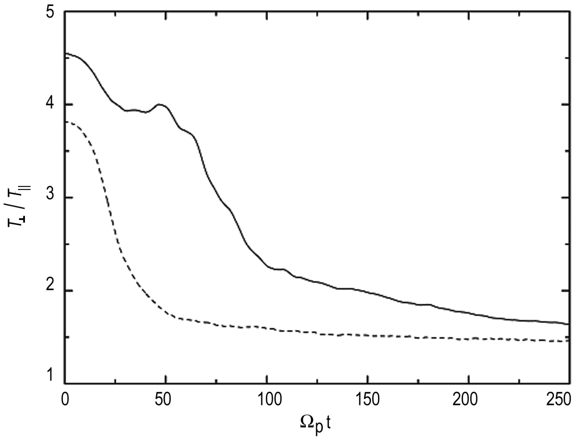

Fig.5 Time evolution of the H^+ and He^{2+} temperature anisotropies for run (b). The solid and dash lines represent He^{2+} and H^+, respectively

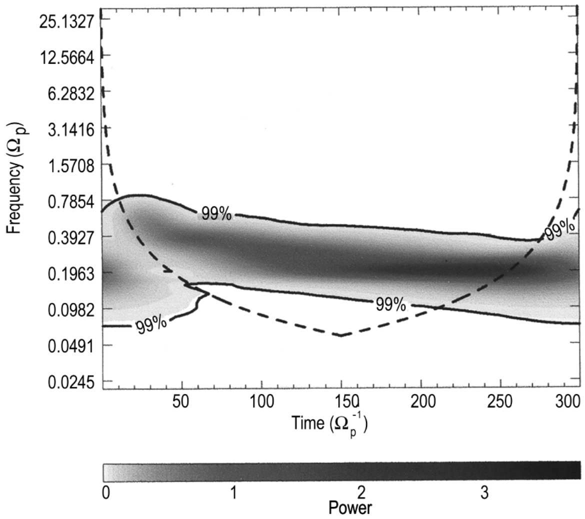

Fig.6 Local wavelet power spectrum of the time series of B_y for run (b)

cyclotron waves dominate the spectrum, while the helium cyclotron waves are negligible. The dominant frequency of the waves is higher than the helium gyrofrequency. The frequencies of the proton cyclotron waves decrease in the nonlinear stage. Then the helium cyclotron waves are excited with a dominant frequency below the helium gyrofrequency, and their frequency band merges with those of the proton cyclotron waves. The spectrum during this period is continuous, which can explain the CON spectral category observed in the PDL. Then the frequencies of the excited waves continue to decrease and form a spectrum with the main power below the helium gyrofrequency, which can explain the LOW category observed in PDL. As in run (a), the polarization of the part of waves is also shown in Fig. 7, which propagate along the $+x$ direction. Obviously, the waves are still left-hand circularly polarized with respect to their propagating direction.

Fig. 8 is the distribution of the frequency at different times for run (b), where A, B, C, and D represent $\Omega_p t = 30$, 80, 150, 220, respectively. At time A, the excited waves are proton cyclotron waves with frequencies

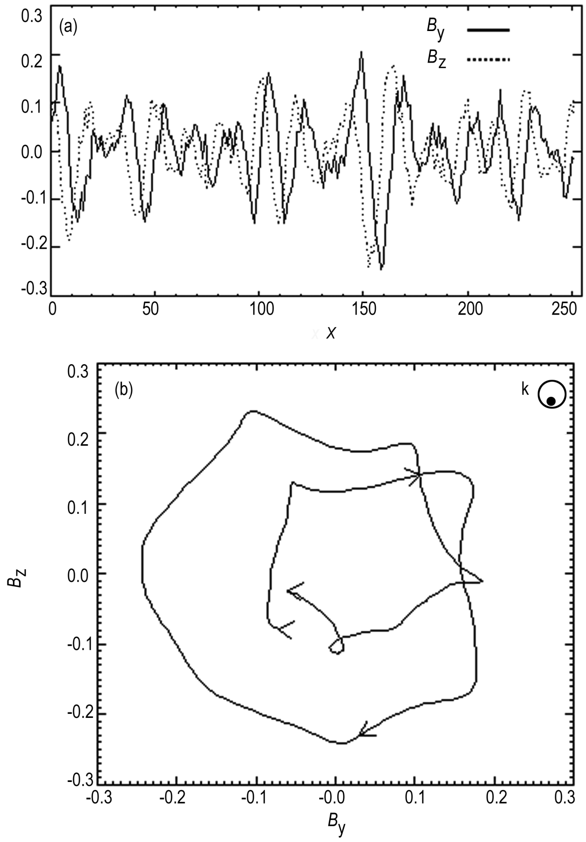

Fig.7 (a) Spatial distribution of the magnetic fields at $\Omega_p t = 80$. (b) Hodograph of the magnetic fields at $nx = 160$ and with the time interval $\Omega_p t$ from 62 to 102

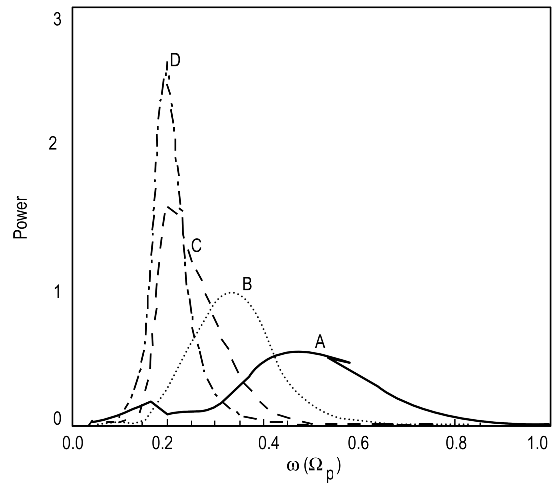

Fig.8 Frequency spectrum of the excited ion cyclotron waves at different times for run (b). The solid(A), dotted(B), dashed(C) and dash-dotted(D) lines represent $\Omega_p t = 30$, 80, 150, 220, respectively

ranging from 0.2 Ω_p to 0.7 Ω_p. Then their frequencies drift to lower values. The helium cyclotron waves with a frequency lower than the helium gyrofrequency are excited at time B, and merge with that of the proton cyclotron waves. Therefore, the spectrum at time A and time B is similar to the CON spectral category observed by AMPTE/CCE. Then the frequencies of the waves continue to drift to lower values at time C and

D. Compared with time C, the wave frequency spectrum at time D becomes narrower and the dominant frequency is around 0.2 Ω_p. Compared with those in Figs. 4 and 8, there is another interesting phenomenon that the dominant frequency of the LOW category decreases with the increase in $\beta_{//p}$.

4 Discussion and conclusions

We performed 1-D hybrid simulations and investigated the spectrum evolution of the ion cyclotron waves excited by the H^+ and He^{2+} temperature anisotropies in a magnetized plasma with the wavelet method. The results show that the proton cyclotron waves and helium cyclotron waves can be excited by the H^+ and He^{2+} temperature anisotropies, respectively. In their linear growing phase, the dominant frequency of the proton cyclotron waves is higher than the helium gyrofrequency (= 0.5 Ω_p), while the dominant frequency of the helium cyclotron waves is lower than the helium gyrofrequency. The proton cyclotron waves are first excited, and then the helium cyclotron waves are excited. The dominant frequency of the proton cyclotron waves can be considered to be nearly a constant for a small $\beta_{//p}$. The BIF category is formed after the helium cyclotron waves are excited. The two peaks of the BIF category are around 0.3 Ω_p and 0.62 Ω_p, which correspond to the dominant frequencies of the helium cyclotron waves and proton cyclotron waves. When $\beta_{//p}$ is large, the wave spectrum becomes broad. The dominant frequency of the proton cyclotron waves decreases in the nonlinear stage, and their frequency band merges with that of the helium cyclotron waves after the helium cyclotron waves are excited, which can explain the CON category observed in the PDL. The LOW category is formed in the quasi-equilibrium stage after the proton cyclotron waves are resonantly absorbed by He^{2+} at low $\beta_{//p}$ or after their frequencies get lower than the helium gyrofrequency for large $\beta_{//p}$.

The dominant frequency of LOW decreases when the increase in $\beta_{//p}$. In summary, the BIF category of the ion cyclotron waves in PDL is formed at low $\beta_{//p}$, while the CON category is generated for a high $\beta_{//p}$. Both the CON and BIF categories are formed just after the helium cyclotron waves are excited. The results obtained are consistent with those of spacecraft observation and linear Vlasov theory [16,17].

References

1 Winske D, Quest K B. 1988, J. Geophys. Res., 93: 9681
2 Gary S P. 1992, J. Geophys. Res., 97: 8519
3 McKean M E, Winske D, Gary S P. 1992, J. Geophys. Res., 97: 19421
4 Liu Y C M, Lee M A, Kucharek H, et al. 2007, J. Geophys. Res., 112: A07217
5 Midgley J E, Davis L. 1963, J. Geophys. Res., 68: 5111
6 Phan T D, Paschmann G, Baumjohann W, et al. 1994, J. Geophys. Res., 99: 121
7 Anderson B J, Fuselier S A, Murr D. 1991, Geophys. Res. Lett., 18: 1955
8 Anderson B J, Fuserlier S A, Gary S P, et al. 1994, J. Geophys. Res., 99: 5877
9 Fuselier S A, Anderson B J, Gary S P, et al. 1994, J. Geophys. Res., 99: 14931
10 Farrugia C J, Gnavi G, Gratton F T, et al. 2004, J. Geophys. Res., 109: A02202
11 Lu Q M, Wang S. 2005, Geophys. Res. Lett., 32: Lo3111
12 Xiao F L, Zhou Q H, He H Y, et al. 2007, J. Geophys. Res., 112: A07219
13 Anderson B J, Fuselier S A. 1993, J Geophys. Res, 98: 1461
14 Hellinger P, Travnicek. 2005, J. Geophys. Res., 110: A04210
15 Samsonov A A, Pudovkin M I, Gary S P, et al. 2001, J. Geophys. Res., 106: 21689
16 Denton R E, Gary S P, Anderson B J, et al. 1994, J. Geophys. Res., 99: 5893
17 Gnavi G, Gratton F T, Farrugia C J. 2000, J. Geophys. Res., 105: 20973
18 Denton R E, Hudson M K, Fuselier S A, et al. 1993, J. Geophys. Res., 98: 13477
19 Cao J B, Mazelle C, Zhou G C. 2000, Phys. Plasma, 7: 696
20 Cao J B, Mazelle C. 2006, Adv. Space Res., 37: 1556
21 Lu Q M, Guo F, Wang S. 2006, J. Geophys. Res., 111: A04207

(Manuscript received 8 July 2008)
(Manuscript accepted 12 November 2008)
E-mail address of GUO Jun: guojun@qust.edu.cn